Optics and Laser Technology 129 (2020) 106271

Contents lists available at ScienceDirect

Optics and Laser Technology

journal homepage: www.elsevier.com/locate/optlastec

Epsilon-near-zero medium for optical switches in Ho solid-state laser at 2.06 μm

Cheng Zhang, Yuqian Zu, Wen Yang, Shouzhen Jiang*, Jie Liu*

Shandong Provincial Engineering and Technical Center of Light Manipulations & Shandong Provincial Key Laboratory of Optics and Photonic Device, School of Physics and Electronics, Shandong Normal University, Jinan 250358, China
Collaborative Innovation Center of Light Manipulations and Applications, Shandong Normal University, 250358, China

HIGHLIGHTS

- The optical properties of ITO nanowires at 2.06 μm were studied for the first time.
- The ITO material was first applied as optical switcher in the 2.06 μm region.
- The passively Q-switched Ho-doped laser based on ITO absorber was achieved.

ARTICLE INFO

Keywords:
Epsilon-near-zero
Indium tin oxide
Optical switch
Passively Q-switched
2.06 μm

ABSTRACT

Indium tin oxide (ITO), an epsilon-near-zero material in the low-dimensional family, was successfully fabricated and first used as an optical switcher in 2.06 μm. In the Tm:fiber pumped passively Q-switched laser, a maximum average output power of 312 mW was obtained with a shortest pulse width of 2.42 μs and a repetition rate of 20.53 kHz, corresponding to a single pulse energy and a peak power of 15.20 μJ and 6.28 W, respectively. Results suggest that ITO is looking forward to develop into a kind of suitable saturable absorber for generation of nanosecond pulse in solid state lasers.

1. Introduction

Solid-state pulse lasers operating in 2.1 μm spectral region have significant applications in numerous fields such as medicine, lidar, spectroscopy, and environmental monitoring [1–3]. Among 2.1 μm laser materials, Ho:YLF crystals have large emission cross section, long upper level lifetime, low quantum loss [4,5]. In addition, it can be directly in-band pumped by 1.9 μm lasers, which bring out merits of low quantum defect and high conversion efficiency [6–8]. With the emergence of high-power Tm-doped fiber lasers, efficient and stabilized Ho:YLF pulse lasers were demonstrated [9,10]. The passively Q-switched (PQS) technology can acquire high peak power and microsecond pulsed laser output by inserting the resonant saturable absorber (SA) absorption characteristics of nonlinearity [11–14]. PQS of Ho:YLF lasers have attracted great attention owing to its simple structure and small size. However, few papers have reported on the PQS Ho:YLF lasers at present [15–17].

In recent years, various low-dimensional materials have brought new opportunities for PQS laser [18–24]. An ENZ (Ɛ∼0) material, in which the real constituent of permittivity vanishes, have drawn broad attention from photonics communities for its potential such as large nonlinearity, near-zero refractive index, decoupling of electricity and magnetism, and infinite phase velocity, was first proposed in the case of metamaterials [25–27]. Large nonlinearity is of particular interest for the nonlinear optics and ultrafast photonics communities. ITO, one of the ENZ materials, has lower carrier density and strong plasmonic absorption peak with broad bandwidth [28,29]. Large optical nonlinearities of ITO with large correlation refractive index and ultrafast recovery time about 360 fs have been reported [30,31]. Besides, ITO can support large doping levels (carrier density as large as $\sim 10^{21}$ cm^{-3}), enabling the ENZ region accurately to localize in the near-infrared and mid-infrared bands [32,33]. Owning to the advantages of wide extent of saturable absorption regions, strong plasmonic absorption peaks, and ultra-fast recovery time, ITO as SA have several researched in 1–2 μm pulsed lasers [34–38]. As far as we know, there is no report on the PQS performance based on ITO of Ho laser around 2.06 μm up to now.

In this paper, we explore an ITO optical switch with excellent

* Corresponding authors at: Shandong Provincial Engineering and Technical Center of Light Manipulations & Shandong Provincial Key Laboratory of Optics and Photonic Device, School of Physics and Electronics, Shandong Normal University, Jinan 250358, China.
E-mail addresses: jiang_sz@126.com (S. Jiang), jieliu@sdnu.edu.cn (J. Liu).

https://doi.org/10.1016/j.optlastec.2020.106271
Received 26 October 2019; Received in revised form 1 April 2020; Accepted 4 April 2020
Available online 10 April 2020
0030-3992/

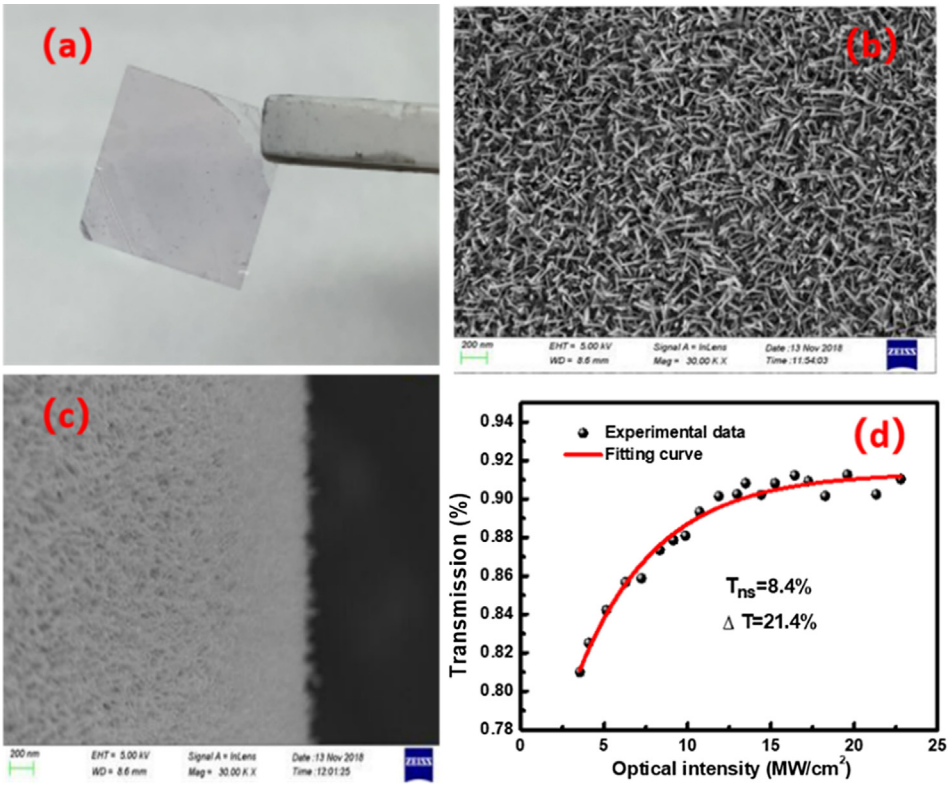

Fig. 1. (a) Fabricated ITO sample on a glass substrate (10 × 10 mm^2); (b) Top-view image of SEM; (c) Side-view image of SEM; (d) Nonlinear absorption property of the ITO.

thermal stability and low insertion loss and first use it as SA in the 2.06 μm region. The in-band pumped PQS mode characteristics were analyzed in detail. This work fully illustrates that ITO was a competitive material as optical switch in mid-infrared pulses laser.

2. Fabrication and characteristics of ITO-SA

ITO was synthesized by carbothermal reduction method on a borosilicate glass substrate with dimensions of 10 × 10 mm^2, as shown in Fig. 1(a). Its color is transparent and slightly brown. Fig. 1(b) shows the top-view scanning electron microscopy (SEM) image of the ITO. It can be seen that there are dense arrays of nanowires with similar size. As shown in the side-view SEM image in Fig. 1(c), the ITO nanowire arrays display a uniform cross section across the entire substrate. The diameter of the ITO nanocrystals is coexistent in the range of 400–500 nm and average diameter is 450 nm. In addition, we measured the nonlinear saturable absorption properties of ITO by a mode-locked Tm-doped fiber laser with a 23.6 ps pulse duration and 31 MHz repetition rate at 2000 nm. The transmittance was detected by varying intensity of the laser seed source power. Fig. 1(d) shows resulting of ITO-SA had a modulation depth of 21.4%. The slightly large modulation depth can improve the damage threshold of the material and make it easy to realize stable pulse trains.

3. Experimental setup

The experimental arrangement for the ITO-based Q-switching of Ho:YLF laser is shown schematically in Fig. 2. The pump source was a commercial Tm:fiber laser (TDFL01-00015) with center wavelength of 1940 nm at 22 °C and maximum power of 30 W with a line width of 0.4 nm (FWHM). A lens with a focal length of 100 mm was used to collimate and focus the pump light into the crystal. To prevent the return of laser to break the Tm:fiber laser, a V-shape stable optical resonator was designed. The 180 mm long laser resonator comprised a

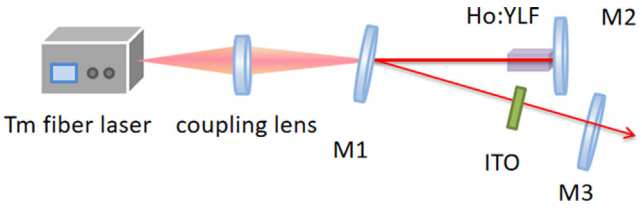

Fig. 2. The schematic of the experimental setup for the PQS operation.

flat pumping mirror M1(T > 99% in the range 1850–1950 nm & R > 99% in the range 2050–2150 nm), flat high-reflective mirror M2(T > 99% in the range 1850–1950 nm & R > 99% in the range 2050–2150 nm), and plano-concave output coupler (OC) M3 with the curvature radius of 200 mm at 1950–2150 nm. The transmittance of OC is 3%. The Ho:YLF laser crystal has a dimension of 3 mm × 3 mm in cross section and 10 mm in length. Both end faces of the crystal are AR coated at 1940 and 2050 nm. The dopant concentrations of 0.5% Ho crystal was chosen to avoid the up-conversion effect caused by high concentration. To increase heat dissipation, the Ho:YLF crystal was wrapped with indium foil and tightly fastened in a water-cooled Cu billet, and the cooling water temperature (accuracy 0.1 ℃) was stable at 13.0 ℃. The radii of TEM00 mode on the laser crystal and SA are calculated by ABCD matrix method approximately 230 and 440 μm, respectively.

4. Results and discussion

The experiment was first conducted on the continuous wave (CW) operation. When the absorbed pump power reached 346 mW, the CW laser began to operate. The maximum output of 1.29 W was acquired under the absorbed pump power of 2.56 W with a slope efficiency of 52.8%. The generated average output power was measured by a power meter (30A-SH-V1, Israel). Then, we inserted ITO into the resonator by

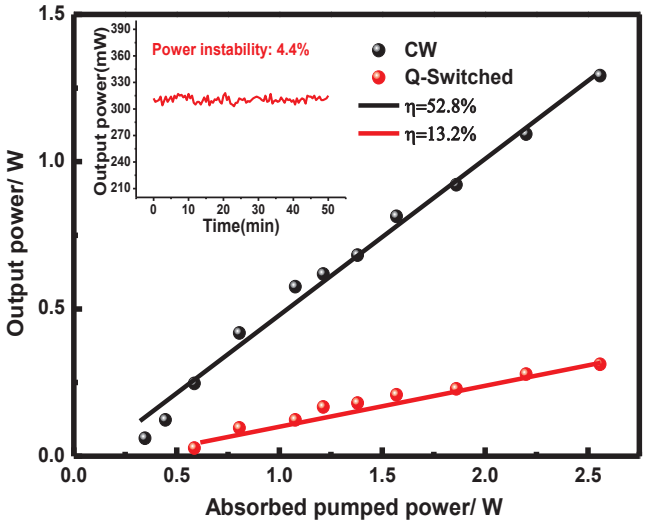

Fig. 3. Output power versus the absorbed pump powers for CW and PQS. The inset figure described instability of maximum output power for 50 min.

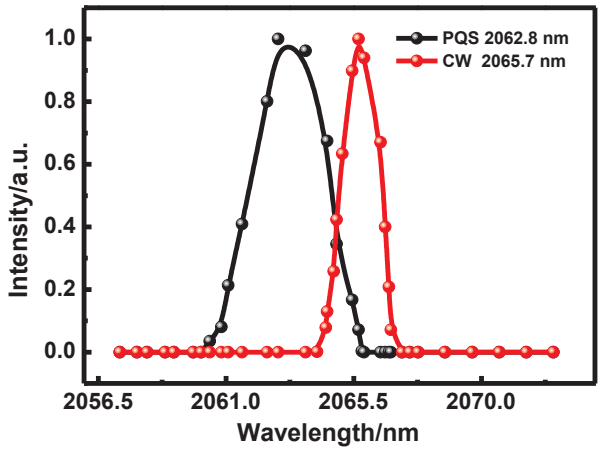

Fig. 4. The output spectra of Ho:YLF laser in CW and PQS regimes.

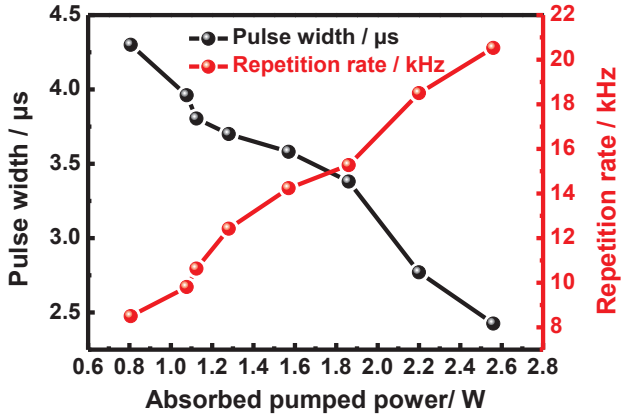

Fig. 5. Pulse duration and repetition rate versus absorbed pump power.

a high precision adjustment frame and calculated the radius of the TEM00 mode at approximately 440 μm by ABCD matrix, which was 20 mm away from the OC. After carefully adjusting the angle and position of ITO, stable PQS operation was achieved with a maximum output power of 312 mW. The output performances of the CW and PQS laser are shown in Fig. 3. As shown in Fig. 3, the value of the laser threshold increased from 346 to 587 mW, whereas the slope efficiency

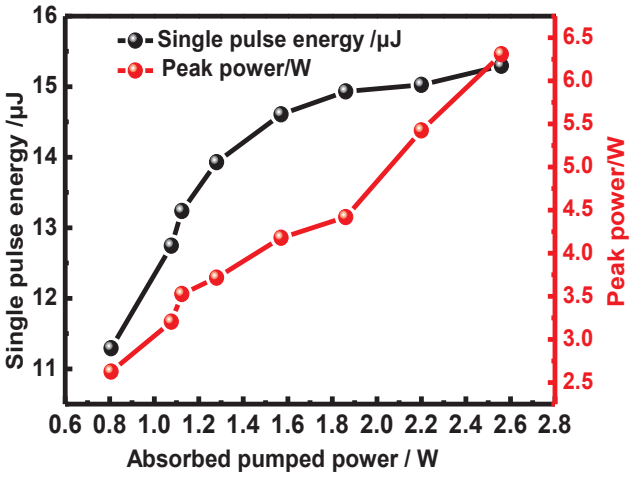

Fig. 6. Single pulse energy and peak power versus absorbed pump power.

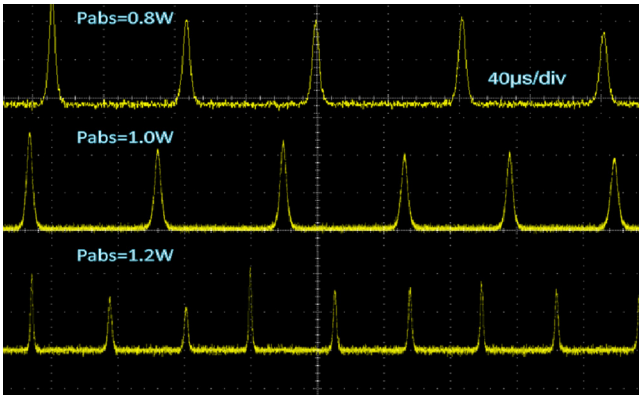

Fig. 7. Q-switched pulse trains under absorbed pump powers of 0.8, 1, and 1.2 W;

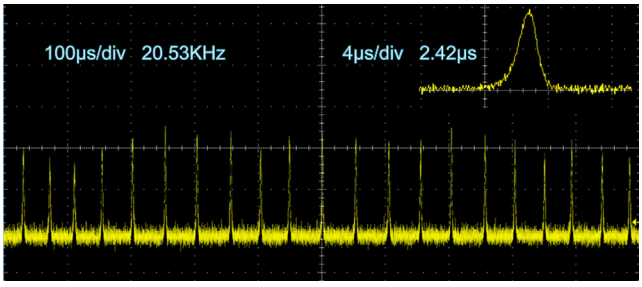

Fig. 8. Oscilloscope display of Q-switched pulse trains at the maximum output power.

decreased from 52.8% to 13.2%. The PQS laser suffered an increase of laser threshold and a decrease of the output power. Compared with CW operation, the reducing of output power and slope efficiency was mainly caused by the inserting loss of SA. Maybe the slope efficiencies are not too high due to inaccurate pump absorption. What's more, the fluctuation of the maximum output power was about 4.4% for 50 min detection, as shown in inset figure. By using a Belarus MS3504i optical spectrum analyzer, as shown in Fig. 4, the output spectra of fiber-pumped Ho:YLF laser were measured in the both CW and PQS regimes. Without SA, the central output wavelength of Ho:YLF laser was located at 2065.7 nm. When the SA was inserted in the cavity, the center output wavelength slightly shifts to 2062.8 nm. This phenomenon was possibly caused by inserting loss of SA and characteristics of quasi-three level laser system.

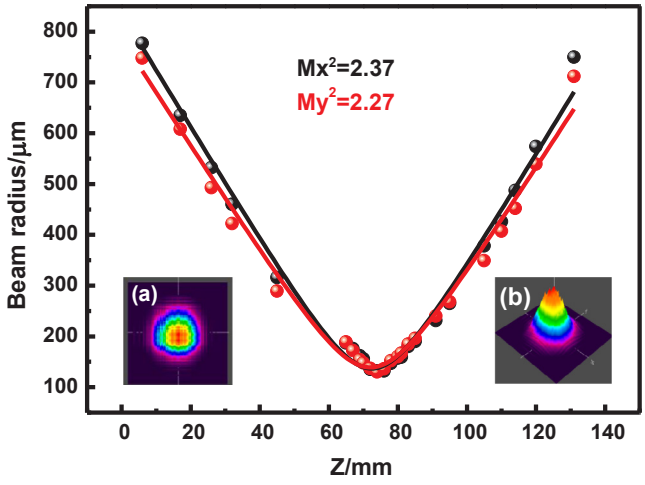

Fig. 9. Beam quality and spatial beam profile.

When the pulse trains were stabilized, the PQS operation was studied in detail. The dependence of the pulse width and pulse repetition rate versus the absorbed pump power is shown in Fig. 5. It can be seen that with the increase of absorbed pump power, the pulse width became narrower and repetition frequency increased. When the absorbed pump power reached 2.56 W, the minimum pulse width was 2.42 μs and maximum repetition rate was 20.53 kHz. Then, we calculated the peak power and single pulse energy, and plotted curves of absorbed pump power. As shown in Fig. 6, the maximum single pulse energy was 15.20 μJ and highest peak power was 6.28 W.

What's more, the typical pulses trains were demonstrated with three different absorbed pump powers, as shown in Fig. 7, which were captured by a 1-GHz digital oscilloscope (model MDO4104C, Tektronix) and a fast photodiode detector (model ET-5000, Electro-Optics). It can be seen clearly that the pulse width decreased with the increase of absorbed pump power at the same time scale. As shown in Fig. 8, a typical stable pulse profile (with the narrowest pulse width) of the PQS laser was obtained. At absorbed pump power of 2.56 W, the beam quality factors of PQS fiber-pumped Ho:YLF laser were measured by the 90/10 knife-edge method. The Ho laser beam was passed through a lens with focal length of 100 mm, and the measured beam radii at different positions were shown in Fig. 9. After fitting of measured data according to the Gauss beam propagation equation, the beam quality factors of PQS fiber-pumped Ho:YLF laser were calculated to be 2.37 and 2.27 in the horizontal and vertical directions, respectively. The laser-beam profile and the 3D light-intensity distribution, as recorded by a detector (PH00435, Model No: NS2-Pyro/9/5-PRO, Photon), are plotted in Fig. 9.

5. Conclusions

In summary, by exploiting the broadband and ultrafast nonlinear optical response of ENZ material of ITO, we first successfully achieved microsecond optical switch in the 2.06 μm region. In the in-band pumped Ho pulse laser with ITO as the SA, the maximum average output power and minimum pulse width were 312 mW and 2.42 μs at a pulse repetition rate of 20.53 kHz. The results suggest the promising potential of ITO as an efficient optical modulator for short-pulse lasers around 2.06 μm. In the future work, by optimizing the parameters of the ITO-SA with low modulation depth and choosing longer crystal, the performance of PQS Ho:YLF laser will be enhanced, resulting in improvement of output power, pulse repetition rate and pulse width.

CRediT authorship contribution statement

Cheng Zhang: Conceptualization, Software, Writing - original draft. **Yuqian Zu:** Methodology, Data curation. **Wen Yang:** Validation, Investigation. **Shouzhen Jiang:** Resources, Project administration. **Jie Liu:** Supervision, Funding acquisition.

Declaration of Competing Interest

This manuscript has not been published or presented elsewhere in part or in entirety and is not under consideration by another journal. We have read and understood your journal's policies, and we believe that neither the manuscript nor the study violates any of these. There are no conflicts of interest to declare.

Acknowledgements

National Natural Science Foundation of China (NSFC) (11974220 and 11674199); Development Projects of Shandong Province Science and Technology (2017GGX30102).

References

[1] T.J. Carrig, Novel pulsed solid-State sources for laser remote sensing, Proc. SPIE 5620 (2004) 187–198.
[2] P.A. Budni, L.A. Pomeranz, M.L. Lemons, C.A. Miller, J.R. Mosto, E.P. Chicklis, Efficient midinfrared laser using 1.9-μm-pumped Ho:YAG and $ZnGeP_2$ optical parametric oscillators, J. Opt. Soc. Am. B 17 (2000) 723–728.
[3] D. Theisen, V. Ott, H.W. Bernd, V. Danicke, R. Keller, R. Brinkmann, Cw high-power IR laser at 2 μm for minimally invasive surgery, Proc. SPIE. 5142–96 (2003).
[4] B.M. Walsh, Review of Tm and Ho Materials; spectroscopy and lasers, Laser Phys. 19 (4) (2009) 855–866.
[5] Y.C. Yin, X.M. Ren, Y. Wang, F.J. Zhuang, J. Li, Z.H. Chang, Generation of high-energy narrowband 2.05 μm pulses for seeding a Ho:YLF laser, Photon. Res. 6 (1) (2018) 1–5.
[6] N. Coluccelli, A. Lagatsky, A.D. Lieto, M. Tonelli, G. Galzerano, W. Sibbett, P. Laporta, Passive mode locking of an in-band-pumped Ho:$YLiF_4$ laser at 2.06 μm, Opt. Lett. 36 (16) (2011) 3209–3211.
[7] E.C. Ji, Q. Liu, M.M. Nie, X.Z. Cao, X. Fu, M.L. Gong, High-slope-efficiency 2.06 μm Ho: YLF laser in-band pumped by a fiber-coupled broadband diode, Opt, Lett. 41 (6) (2016) 1237–1240.
[8] M. Schellhorn, High-energy, in-band pumped Q-switched Ho^{3+}:$LuLiF_4$ 2 μm laser, Opt. Lett. 35 (15) (2010) 2609–2611.
[9] M. Schellhorn, A comparison of resonantly pumped Ho:YLF and Ho:LLF lasers in CW and Q-switched operation under identical pump conditions, Appl. Phys. B 103 (4) (2011) 777–788.
[10] A. Dergachev, P.F. Moulton, T.E. Drake, High-power, high-energy Ho:YLF laser pumped with Tm: fiber laser, Adv. Solid-State Photon. 608 (2005).
[11] X.T. Yang, Y.L. Mu, N.B. Zhao, Ho:SSO solid-state saturable-absorber Q switch for pulsed Ho:YAG laser resonantly pumped by a Tm:YLF laser, Opt. Laser Technol. 107 (2018) 398–401.
[12] C. Zhang, J. Liu, X.W. Fan, Q.Q. Peng, X.S. Guo, D.P. Jiang, X.B. Qian, L.B. Su, Compact passive Q-switching of a diode-pumped Tm, Y:CaF_2 laser near 2μm, Opt. Laser Technol. 103 (2018) 89–92.
[13] X.M. Duan, W.M. Lin, Y. Ding, B.Q. Yao, T.Y. Dai, J. Li, Y.B. Pan, L.J. Li, "High-power resonantly pumped passively Q-switched Ho:$GdVO_4$ laser, Appl. Phys. B 122 (1) (2016) 22.
[14] J.J. Liu, H. Huang, F. Zhang, Z. Zhang, J. Liu, H. Zhang, L.B. Su, Bismuth nanosheets as a Q-switcher for a mid-infrared erbium-doped SrF_2 laser, Photon. Res. 6 (2018) 762–767.
[15] C. Yang, Y.L. Ju, B.Q. Yao, T.Y. Dai, X.M. Duan, J. Li, Y. Ding, W. Liu, Y.B. Pan, C.Y. Li, Passively Q-switched Ho:YLF laser pumped by Tm^{3+}-doped fiber laser, Opt. Laser Technol. 77 (2016) 55–58.
[16] B.Q. Yao, X.L. Li, Z. Cui, T.Y. Dai, S. Bai, H.Y. Yang, X.M. Duan, Y.L. Ju, "High-repetition rate passively Q-switched Ho:YLF laser with graphene as a saturable absorber, Opt. Eng. 54 (7) (2015) 076105.
[17] Z. Cui, B.Q. Yao, X.M. Duan, J. Li, S. Bai, X.L. Li, Y. Zhang, J.H. Yuan, T.Y. Dai, Y.L. Ju, C.Y. Li, Y.B. Pan, Experimental study on a passively Q-switched Ho:YLF laser with polycrystalline Cr^{2+}:ZnS as a saturable absorber, Chin. Phys. Lett. 32 (08) (2015) 84205.
[18] Z.Q. Li, R. Li, C. Pang, N.N. Dong, J. Wang, H.H. Yu, F. Chen, 8.8 GHz Q-switched mode-locked waveguide lasers modulated by $PtSe_2$ saturable absorber, Opt. Express 27 (2019) 8727–8737.
[19] Y.Q. Zu, C. Zhang, X.S. Guo, W.Y. Liang, J. Liu, L.B. Su, H. Zhang, A solid-state passively Q-switched Tm, Gd:Ca_F2 laser with a $Ti_3C_2T_x$ MXene absorber near 2 μm, Laser Phys. Lett. 16 (2019) 015803.
[20] J.J. Liu, X.Y. Feng, X.W. Fan, Z. Zhang, B. Zhang, J. Liu, L.B. Su, Efficient continuous-wave and passive Q-switched mode-locked Er^{3+}:CaF_2-SrF_2 lasers in the mid-infrared region, Opt. Lett. 43 (10) (2018) 2418–2421.
[21] Y.P. Yao, N. Cui, Q.G. Wang, L.L. Dong, S.D. Liu, D.L. Sun, H.Y. Zhang, D.H. Li, B.T. Zhang, J.L. He, Highly efficient continuous-wave and $ReSe_2$ Q-switched ~3 μm dual-wavelength Er:YAP crystal lasers, Opt. Lett. 44 (11) (2019) 2839–2842.

[22] X.Y. Feng, B.Y. Ding, W.Y. Liang, F. Zhang, T.Y. Ning, J. Liu, H. Zhang, MXene $Ti_3C_2T_x$ absorber for a 1.06 μm passively Q-switched ceramic laser, Laser Phys. Lett. 15 (2018) 085805.
[23] Z.Q. Li, Y.X. Zhang, C. Cheng, H.H., F. Chen, 6.5 GHz Q-switched mode-locked waveguide lasers based on two-dimensional materials as saturable absorbers, Opt. Express 26 (2018) 11321–11330.
[24] C. Li, J. Liu, Z.N. Guo, H. Zhang, W.W. Ma, J.Y. Wang, X.D. Xu, L.B. Su, Black phosphorus saturable absorber for a diode-pumped passively Q-switched Er:CaF_2 mid-infrared laser, Opt. Commun. 406 (2018) 158–162.
[25] N. Engheta, Pursuing near-zero response, Science 340 (6130) (2013) 286–287.
[26] B. Edwards, A. Alù, M.E. Young, M. Silveirinha, N. Engheta, "Experimental verification of epsilon-near-zero metamaterial coupling and energy squeezing using a microwave waveguide, Phys. Rev. Lett. 100 (2008) 033903.
[27] I. Liberal, N. Engheta, Near-zero refractive index photonics, Nat. Photon. 11 (2017) 149–158.
[28] X.G. Liu, J. Park, J.H. Kang, H.T. Yuan, Y. Cui, H.Y. Hwang, M.L. Brongersma, Quantification and impact of nonparabolicity of the conduction band of indium tin oxide on its plasmonic properties, Appl. Phys. Lett. 105 (18) (2014) 181117.
[29] Y.L. Gui, M. Miscuglio, Z.Z. Ma, M.H. Tahersima, S.A. Sun, R. Amin, H. Dalir, Volker J. Sorger, Towards integrated metatronics: a holistic approach on precise optical and electrical properties of indium tin oxide, Sci. Rep. 9 (1) (2019) 1–10.
[30] M.Z. Alam, I. De Leon, R.W. Boyd, Large optical nonlinearity of indium tin oxide in its epsilon-near-zero region, Science 352 (6287) (2016) 795–797.
[31] Q.B. Guo, Y.D. Cui, Y.H. Yao, Y.T. Ye, Y. Yang, X.M. Liu, S.A. Zhang, X.F. Liu, J.R. Qiu, H. Hosono, Exploiting ITO colloidal nanocrystals for ultrafast pulse generation, arXiv preprint 1701.07586, 2017.
[32] J. Lee, M.S. Kwon, Mid-infrared optical waveguide modulator based on the epsilon-near-zero effect of ITO, in: 2015 11th Conference on Lasers and Electro-Optics Pacific Rim (CLEO-PR). IEEE, 3, 2015, 1–2.
[33] Y. Wang, A.C. Overvig, S. Shrestha, R. Zhang, R. Wang, N.F. Yu, L.D. Negro, Tunability of indium tin oxide materials for mid-infrared plasmonics applications, Opt. Mater. Express 7 (8) (2017) 2727–2739.
[34] Z.M. Zhang, J.J. Liu, Q.Q. Hao, J. Liu, Sensitive saturable absorber and optical switch of epsilon-near-zero medium, Appl. Phys Express 12 (6) (2019).
[35] X.T. Jiang, H.L. Lu, Q. Li, H. Zhou, S.D. Zhang, H. Zhang, Epsilon-near-zero medium for optical switches in a monolithic waveguide chip at 1.9 μm, Nanophotonics 7 (11) (2018) 1835–1843.
[36] J. Guo, H.N. Zhang, C. Zhang, Z. Li, Y.Q. Sheng, C.H. Li, X.H. Bao, B.Y. Man, Y. Jiao, S.Z. Jiang, Indium tin oxide nanocrystals as saturable absorbers for passively Q-switched erbium-doped fiber laser, Opt. Mater. Express 7 (10) (2017) 3494–3502.
[37] Q.X. Guo, J. Pan, D.W. Li, Y.M. Shen, X.L. Han, J.J. Gao, B.Y. Man, H.N. Zhang, S.Z. Jiang, Versatile mode-locked operations in an Er-doped fiber laser with a film-type indium tin oxide saturable absorber, Nanomaterials 9 (5) (2019) 701.
[38] J.Y. Wu, L. Qian, Propagation of ultrashort pulses in indium tin oxide epsilon-near-zero subwavelength metamaterial at 2 μm, Laser Sci.. Opt. Soc. Am. JTu3A.28 (2019).